International Journal of Nanomedicine

Dovepress
open access to scientific and medical research

Open Access Full Text Article

ORIGINAL RESEARCH

Effect of *Lonicerae japonicae* Flos Carbonisata-Derived Carbon Dots on Rat Models of Fever and Hypothermia Induced by Lipopolysaccharide

This article was published in the following Dove Press journal:
International Journal of Nanomedicine

Jiashu Wu[1]
Meiling Zhang[1]
Jinjun Cheng[1]
Yue Zhang[2]
Juan Luo[1]
Yuhan Liu[1]
Hui Kong[1]
Huihua Qu[3]
Yan Zhao[1]

[1]School of Traditional Chinese Medicine, Beijing University of Chinese Medicine, Beijing 100029, People's Republic of China; [2]School of Science Life, Beijing University of Chinese Medicine, Beijing 100029, People's Republic of China; [3]Center of Scientific Experiment, Beijing University of Chinese Medicine, Beijing 100029, People's Republic of China

Introduction: A correlation is established between the efficacy of Chinese herbal medicine and its charcoal drugs. *Lonicerae japonicae* Flos (LJF) is commonly used to treat fever, carbuncle, and tumors, among others. LJF Carbonisatas (LJFC) is preferred for detoxifying and relieving dysentery and its related symptoms. However, the mechanisms underlying the effects of LJFC remain unknown.

Aim: The aim of this study was to explore the effects of LJFC-derived carbon dots (LJFC-CDs) on lipopolysaccharide (LPS)-induced fever and hypothermia rat models.

Methods: LJFC-CDs were characterized using transmission electron microscopy, high-resolution transmission electron microscopy, Fourier-transform infrared, ultraviolet, fluorescence, X-ray photoelectron spectroscopy, X-ray diffraction and high-performance liquid chromatography. The anti-inflammatory effects of LJFC-CDs were evaluated and confirmed using rat models of LPS-induced fever or hypothermia.

Results: The LJFC-CDs ranged from 1.0 to 10.0 nm in diameter, with a yield of 0.5%. LJFC-CDs alleviated LPS-induced inflammation, as demonstrated by the expression of tumor necrosis factor-α, interleukin (IL)-1β, and IL-6 and the recovery of normal body temperature.

Conclusion: LJFC-CDs may have an anti-inflammatory effect and a potential to alleviate fever and hypothermia caused by inflammation.

Keywords: carbon dots, *Lonicerae japonicae* Flos, anti-inflammatory, lipopolysaccharide

Introduction

In recent years, research into nanotechnology has increased. Carbon dots (CDs) are a novel member of the carbon nanomaterial family that are biocompatible and have excellent photoluminescence, high electron transfer capability, low toxicity, and versatile surface engineering properties.[1] CDs have been widely applied in biomedical science, including use as a probe for in vivo imaging,[2] a material for bone regeneration,[3] nanocarriers for drugs, therapeutic genes, photosensitizers, and antibacterial nanomaterials molecules.[4] Additionally, nanomaterials have shown great potential in treatment of diseases.[5] We have studied the therapeutic effects of CDs of drugs used in traditional Chinese medicine (TCM).

Lonicerae japonicae Flos (LJF), named Jin Yinhua in Chinese, has a long history of use in China. *The Pharmacopoeia of the People's Republic* stipulates that LJF is the dried flower bud or the first-blooming flower of *L. japonica* Thunb of Caprifoliaceae.[6] LJF was first documented as the flower feature of Lonicera in the *Xin Xiu Ben Cao* of

Correspondence: Yan Zhao
Tel +86 010 6428 6705
Fax +86 1 6428 6821
Email zhaoyandr@163.com

submit your manuscript | www.dovepress.com
DovePress
http://doi.org/10.2147/IJN.S248467

the Tang Dynasty,[7] while the name of Jin Yinhua first appeared in *Su Shen Liang Fang* of the Song Dynasty.[8]

LJF is a commonly used drug in TCM and is often made into a charcoal processed product for use. LJF Carbonisatas (LJFC) is preferred for detoxifying (relieve fever, inflammation and other symptoms) and relieving dysentery. However, the mechanism underlying the action of LJFC is not clear.

Lipopolysaccharide (LPS), a component of Gram-negative bacteria, is often used to establish rat models of systemic inflammatory and fever. LPS can trigger autonomic and behavioral thermoeffector responses, and induce either fever or hypothermia depending on the dose and ambient temperature.[9] Low doses of LPS can result in fever, whereas high doses can lead to hypothermia, although more studies have focused on LPS-induced fever. Different doses of LPS can have differential effects on body temperature, suggesting that the same pathogenic factor can affect thermoregulation in different ways. This situation is most likely caused by inflammation.

In this study, we identified and characterized LJFC-CDs. The experimental process is shown in Figure 1. Furthermore, we evaluated the effect of LJFC-CDs on LPS-induced rat models of fever and hypothermia.

Materials and Methods

Chemicals

LJF was purchased from Beijing Qiancao Traditional Chinese Medicine Co., Ltd, (Beijing, China), and LJFC was prepared in our laboratory. LPS, from Escherichia coli 055:B5 purified by phenol extraction, was purchased from Sigma Chemical (St Louis, MO, USA). Dialysis membranes (cat. no.: HF132640-1m, molecular weight 1000 Daltons, flat width: 45 mm) were obtained from Beijing Ruida Henghui Technology Development Co., Ltd, (Beijing, China). A cell counting kit-8 (CCK-8) was obtained from Dojindo Molecular Technologies, Inc. (Kumamoto, Japan). All other commercial chemicals and reagents used in this study were of analytical reagent grade and were obtained from Sinopharm Chemical Reagents Beijing (Beijing, China). All experiments were conducted using deionized water.

Animals

The study's protocols were in accordance with the Guide for the Care and Use of Laboratory Animals and were approved by the Committee of Ethics of Animal Experimentation of the Beijing University of Traditional Chinese Medicine. Male adult Sprague–Dawley (SD) rats (weighing 220.0 ± 10.0 g) were purchased from the Laboratory Animal Center, Si Beifu. All animals were placed in a controlled environment with room temperature of 24.0 ± 1.0°C, relative humidity of 55–65%, and a 12 h light/dark cycle, with free access to food and water, adaptive feeding for 7 days.

Preparation of LJFC-CDs

LJF (280 g) was placed in a crucible and covered with aluminum foil to form a seal. Then, the LJF was calcined at 350°C for 1 h in a muffle furnace (TL0612 muffle furnace; Beijing ZhongKe Aobo Technology Co., Ltd; Beijing, China). After cooling, the LJFC in the crucibles was ground into a fine powder. One-hundred grams of powder was removed, mixed with 3 L of deionized water, and boiled twice in a water bath for 1 h each time. The residue was removed by filtration through a 0.22 μm filter membrane and the solution was concentrated and dialyzed (1 kDa molecular

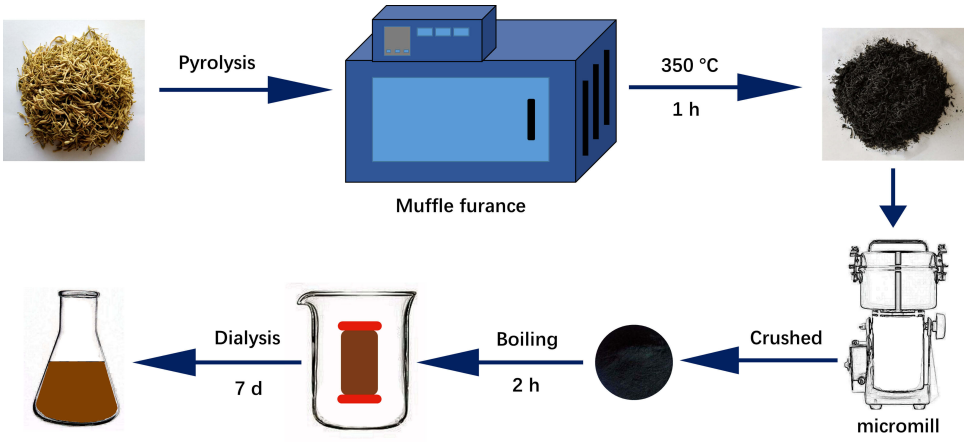

Figure 1 Flowchart for the preparation of *Lonicerae japonicae* Flos carbonisata-derived carbon dots (LJFC-CDs).

weight cut-off) against deionized water for 168 h. The process of LJFC-CD preparation is shown in Figure 1.

Characterization of LJFC-CDs

The morphology of LJFC-CDs was characterized using a TEM operating at an acceleration voltage of 200 kV, with a Tecnai G220 (FEI Company, USA). The structural details and atomic lattice fringes of the LJFC-CDs were examined using HRTEM with a JEN-1230 (Japan Electron Optical Laboratory, Tokyo, Japan). The photoluminescent spectra were recorded using a F-4500 fluorescence spectrophotometer (Hitachi, Tokyo, Japan) and the UV–vis absorption spectra were measured by UV–vis spectroscopy (CECIL, Cambridge, UK) in a standard quartz cuvette. FTIR spectroscopy was performed using a FTIR spectrophotometer (Thermo Fisher, CA, USA) with a spectral window between 400 and 4000 cm^{-1}. The surface composition of the CDs was evaluated using XPS (ESCALAB 250Xi; Thermo Fisher Scientific, Waltham, MA, USA) with a monochromatic Al Kα x-ray source. XRD was measured using a D8 DISCOVER Plus x-ray Diffractometer with Cu K α radiation.

Quantum Yield of LJFC-CDs

Quinine sulphate (quantum yield [QY], 54% in 0.1 M sulfuric acid [H_2SO_4]) was used as a reference to determine the QY of the LJFC-CDs, and was calculated using the following formula:

$$Q_{CDs}=Q_R \times \frac{I_{CDs}}{I_R} \times \frac{A_R}{A_{CDs}} \times \frac{\eta^2_{CDs}}{\eta^2_R}$$

Where Q is QY; I is the measured comprehensive emission intensity; A is the absorbance at the excitation wavelength and η is the refractive index of the solvent. CDs and R represent the LJFC-CDs and reference, respectively. To reduce the influence of reabsorption, A_R and A_{CDs} were kept below 0.05.

LJFC-CDs Fingerprint Analysis

LJF and LJFC-CDs were compared and analyzed by HPLC to evaluate their individual components before and after pyrolysis and dialysis. HPLC was performed using a 1260 HPLC (Agilent, Waldbrand, Germany) equipped with a column compartment, autosampler, degasser, quaternary pump, and diode-array detector, using a ZORBAX-C18 column (250 × 4.6 × 5 mm, Orochem Technologies, Naperville, IL, USA). Methanol extract of LJF, LJFC-CDs, and chlorogenic acid (LJF index component) was prepared and processed under the same detection conditions.

An aliquot (10 μL) was injected into a ZORBAX-C18 column and eluted at 23°C for HPLC analysis. The mobile phase consisted of acetonitrile (solution A) and 4% phosphoric acid (solvent B). These two solutions were filtered through 0.22 μm cellulose acetate membrane filters (Jin Teng, Tianjin, China) before use. The gradient program was as follows: 0–15 min, 10–20% A and 90–80% B; 15–30 min, 20% A and 80% B; 30–40 min, 20–30% A and 80–70% B; 40–50 min, 30–10% A and 70–90% B. The column was held at 35°C. The flow rate was 1.0 mL/min, and the detection wavelength was 327 nm.

Cytotoxicity Assessment: CCK-8 Assay

The cytotoxicity of LJFC-CDs was evaluated via a TCCK-8 assay using RAW 264.7 cells (Ke Bai, Nanjing, China). The cells were cultured in Dulbecco's modified Eagle's medium (DMEM), supplemented with 20% fetal bovine serum, in a moist 5% CO_2 atmosphere at 37°C. Cells were counted and then seeded in a 96-well plate at a density of 1 × 10^4 cells per well. After a 24 h incubation, the original medium in each well was discarded, different concentrations of LJFC-CDs were added (2000, 1000, 500, 250, 125, 62.5, 31.25, 15.62, 7.81, and 3.90 μg/mL), and cells were incubated for a further 24 h. Cells were washed with phosphate-buffered saline to remove excess LJFC-CDs and media. Then, 10 μL of CCK-8 solution was mixed with 100 μL of culture medium, and then added to each well for 2 h incubation. Using a microplate reader (Bitoke, VT, USA), the optical density of each well was determined at a wavelength of 450 nm, using pure DMEM as a blank. Untreated cells were used as controls. Cell viability was measured using the following formula:

$$\text{Cell viability(\% of control)}=\frac{A_e-A_b}{A_c-A_b} \times 100$$

Ae, Ab, and Ac corresponded to the absorbance of experimental, blank, and control groups, respectively.

LPS-Induced Rat Models with Abnormal Temperature and Drug Treatment

Anal temperature of rats was measured with an electronic thermometer (Omron co., Ltd, Dalian, China) every day for 3 consecutive days before modeling, and the average body temperature of three days was taken as baseline. LPS was used to establish models of abnormal body temperature in rats. Male SD rats (n = 40) were weighed and randomly divided into five groups (each n = 8) as follows: control (NS 5 mL/kg, i.p; NS 5 mL/kg, p.o.); fever model (LPS 20

μg/kg, i.p; NS 5 mL/kg, p.o.); hypothermia model (LPS 500 μg/kg, i.p; NS 5 mL/kg, p.o.); fever treatment (LPS 20 μg/kg, i.p; LJFC-CDs 0.18 mg/kg, p.o.); hypothermia treatment (LPS 500 μg/kg, i.p; LJFC-CDs 0.18 mg/kg, p.o.). Models of fever and hypothermia were developed by injecting rats with different doses of LPS. The treatment groups were administered LJFC-CDs orally to evaluate the effect of LJFC-CDs on the SD rat models of fever and hypothermia. The anal temperature of rats was measured at 0.5, 1, 2, 3, and 4 h with an electronic thermometer.

Detection of Cytokines in Serum

After temperature determination at different times, all rats were anesthetized with pentobarbital sodium (30 mg/kg). Blood samples were collected from rats via the abdominal aorta by blood taking needles (Shandong Junnuo co., Ltd, Heze, China) and vacuum blood collection tubes (Becton Dickinson Medical Instrument co., Ltd, Shanghai, China). Blood samples were maintained at room temperature for 60 min, after which serum was separated from whole blood by centrifugation at 3000 rpm for 15 min at 4°C. The levels of TNF-α, IL-1β, and IL-6 in serum from rats were determined by ELISA (Cloud-Clone Crop Technology co., Ltd., Wuhan, China), following the manufacturer's instructions.

Detection of PGE_2 and cAMP in PO/AH

After blood samples were obtained, PO/AH samples were taken from the brain following decapitation, and then weighed. Rat PO/AH tissues were added to PBS (pH 7.4) in equal proportions in an ice bath, and the samples were homogenized with a portable high speed disperser (Ningbo Xinzhi co., Ltd., Ningbo, China), centrifuged for 20 min (3000 rpm) at 4°C, and the supernatant was stored at −80°C for later use. The levels of PGE_2 and cAMP in PO/AH suspensions were determined by ELISA (Cloud-Clone Crop Technology Co., Ltd., Wuhan, China), according to the manufacturer's instructions.

Statistical Analysis

Data were analyzed using IBM SPSS Statistics for Windows 21.0 (SPSS Inc., Chicago, IL, USA) data. The mean ± standard deviation was used for data with normal distribution and uniform variance. One-way analysis of variance (ANOVA), with a least significant difference (LSD) test, was used for multiple comparisons. $p < 0.05$ was considered to denote statistical significance.

Results

Characterization of LJFC-CDs

The morphology and particle size distribution of LJFC-CDs were determined by transmission electron microscope (TEM) and high solution TEM (HRTEM) for determination of nanostructure. TEM images showed that the LJFC-CDs were almost spherical (Figure 2A), with a favorable degree of separation, and a size distribution range of 1.0–10.0 nm (Figure 2B). Additionally, HRTEM showed that the lattice spacing of LJFC-CDs was 0.290 nm (Figure 2C).

The fluorescence spectra of LJFC-CDs revealed maximum emission at 464 nm and maximum excitation at 384 nm (Figure 3A). As shown in Figure 3B, the ultraviolet-visible (UV–vis) absorption spectrum showed that the LJFC-CDs had a wide absorption spectrum, without any evident peak. The yield of LJFC-CDs was 0.5%.

Fourier transform infrared (FTIR) spectra of the purified LJFC-CDs are shown in Figure 3C, and exhibited characteristic peaks at 3432, 2922, 1637, 1384, 1111, and 519 cm^{-1}. These were associated with O-H groups; C-H groups, where weak absorption was assigned to the stretching of methylene groups; the absorption peak, which was the characteristic absorption of C=O bend; C-N, N-H, and COO groups; weak C-O stretching bend; and O-H stretch, respectively. The X-ray diffraction (XRD) profiles showed that the LJFC-CD (Figure 3D) diffraction peak was located at 22.765°, and the atomic lattice fringe value was 0.3903. This result is similar to that in our previous report.[10]

X-ray photoelectron spectroscopy (XPS) was used to characterize the surface composition and elements of LJFC-CDs. As shown in Figure 4A, the LJFC-CDs were composed of 73.15% carbon, 23.16% oxygen, and 1.84% nitrogen. Three typical peaks were present in the XPS spectrum: 284.7, 399.6, and 532.2 eV, corresponding to the characteristic binding energy signals of C 1s, N 1s, and O 1s, respectively. The C 1s (Figure 4B) spectrum could be divided into four component peaks: 284.3 eV (sp^2 C), 284.9 eV (C-N), 285.7 eV (C=O), and 288.6 (C-O). The O 1s (Figure 4C) peak was mainly composed of two subpeaks at 531.8 eV (C-O) and 533.2 eV (C=O). Two peaks at 399.4 and 400.6 eV were shown in the spectrum of N 1s (Figure 4D), which were assigned to C-N, and N-H.

HPLC Profile of LJF and LJFC-CDs

LJF and LJFC-CDs were compared by high-performance liquid chromatography (HPLC) (Figure 5). Chlorogenic acid was found in the LJF solution. Conversely, no active

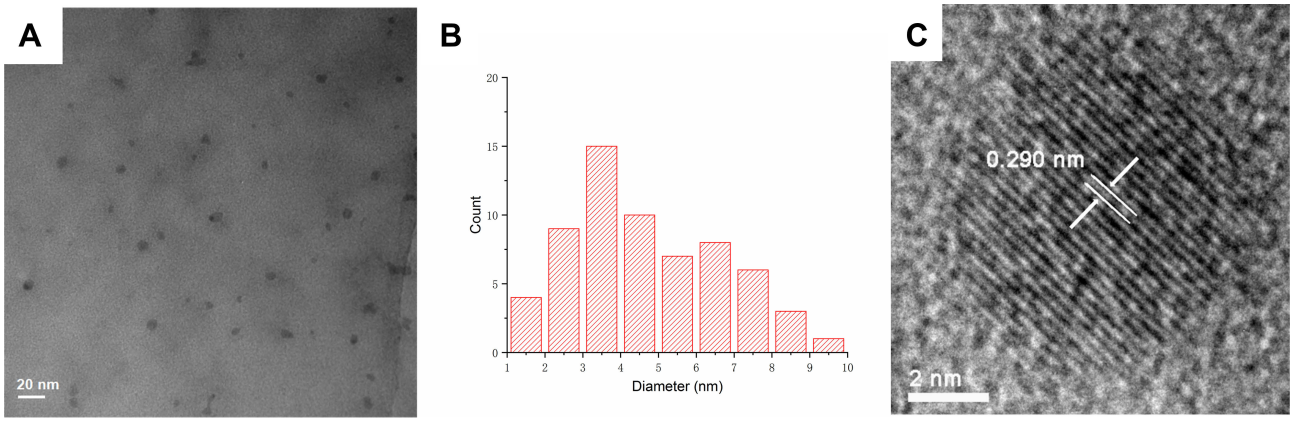

Figure 2 (**A**) Transmission electron microscope (TEM) images of *Lonicerae japonicae* Flos carbonisata-derived carbon dots (LJFC-CDs) displaying ultra-small particles. (**B**) Histogram depicting particle size distribution. (**C**) High-resolution TEM (HRTEM) image of LJFC-CDs.

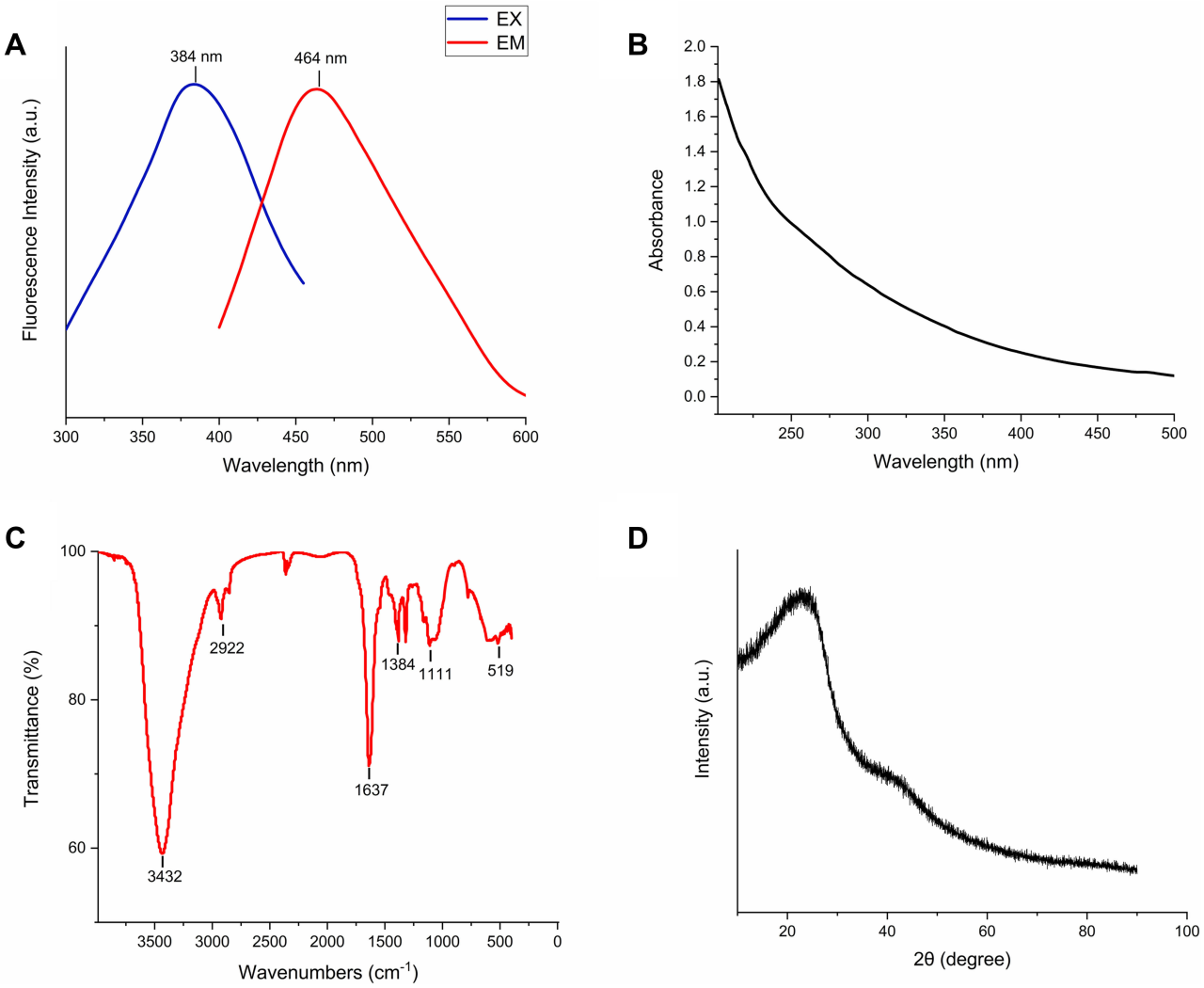

Figure 3 (**A**) Fluorescence spectra for excitation and emission. (**B**) Ultraviolet–visible (UV–vis) spectrum of LJFC-CDs. (**C**) FTIR spectrum of LJFC-CDs. (**D**) X-ray diffraction pattern of LJFC-CDs.

small molecule compounds were identified in the prepared LJFC-CDs solution.

Cellular Toxicity

LJFC-CDs ranging from 3.91 to 2000 μg/mL were evaluated (Figure S1). LJFC-CDs were found to promote activity of RAW 264.7 cells at concentrations as high as 500 μg/mL. At a concentration of 15.63 μg/mL, the maximum activity rate of RAW 264.7 cells was 148%. In contrast, when the concentration was 1000–2000 μg/mL, the viability of RAW 264.7 cells decreased. This indicates that the cytotoxicity of LJFC-CDs is negligible at a concentration of 500 μg/mL.

Effect of LJFC-CDs on Body Temperature of LPS-Treated Rats

As shown in Figure 6, i.p. injection of high-dose LPS (500 μg/kg) induced hypothermia in rats, while i.p. injection of low-dose LPS (20 μg/kg) induced fever. Thirty minutes after LPS injection, the average body temperature of rats in the fever model (FM) group increased by approximately 0.5°C, indicating that the LPS dose used was successful at inducing fever. After 3 h, body temperature peaked, and increased by an average 1°C overall. At 4 h, body temperature had decreased, but remained 0.5°C higher than the baseline temperature. Conversely, body temperature of animals in the hypothermia model (HM) group tended to decrease. After 2 h, body temperature had decreased by about 0.67°C, indicating that the model was successful at causing hypothermia. After 4 h, temperature remained about 1°C lower than the baseline. Although the body temperature of rats in the control group fluctuated, the increase and decrease did not exceed 0.3°C. Similarly, there were no apparent fluctuations in the body temperature of animals in the fever treatment (FT) and hypothermia treatment (HT) groups treated with LJFC-CDs.

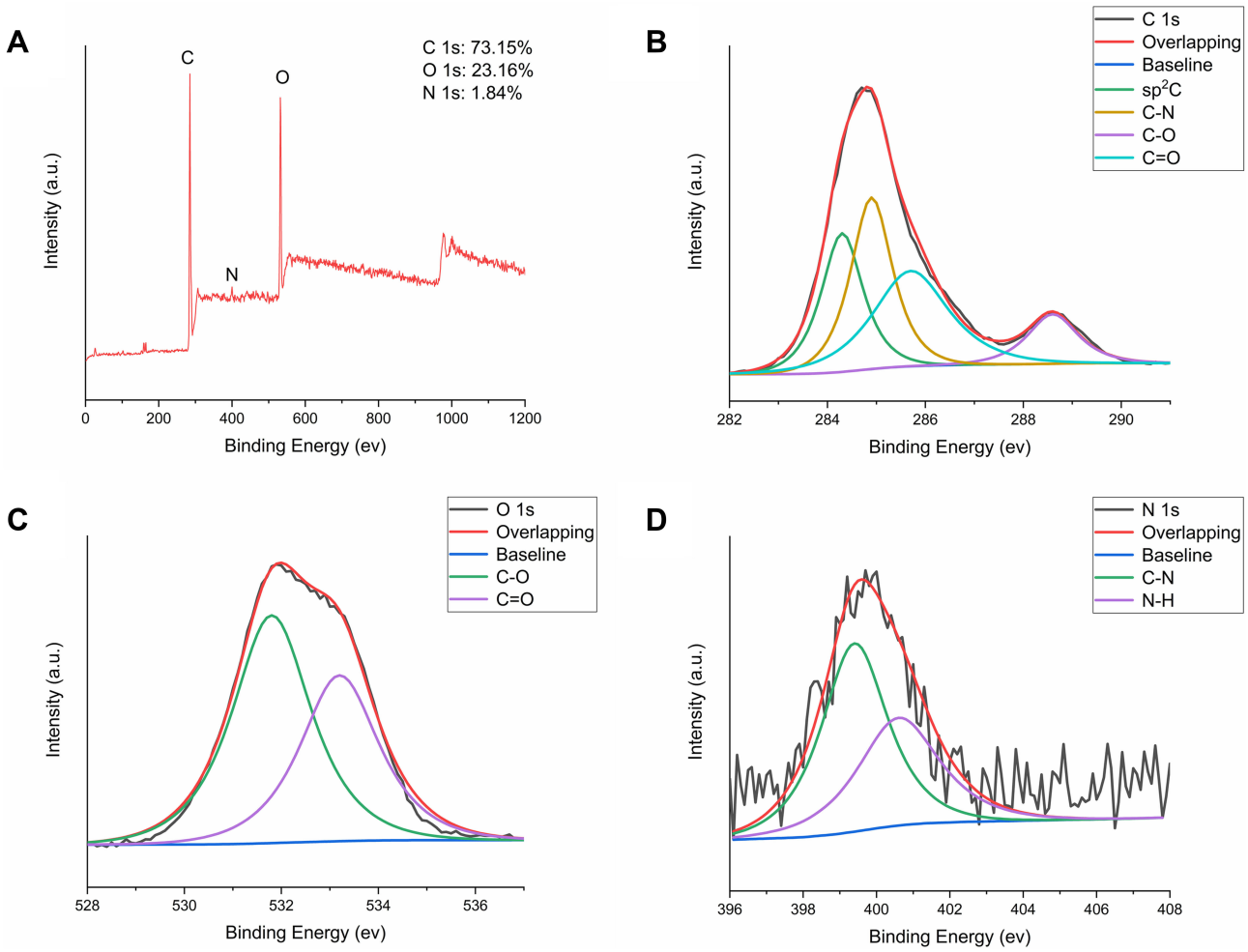

Figure 4 (**A**) Full-scan x-ray photoelectron spectroscopy (XPS) survey spectra of LJFC-CDs. (**B**) C 1s, (**C**) O 1s, and (**D**) N 1s high-resolution x-ray photoelectron spectroscopy spectra.

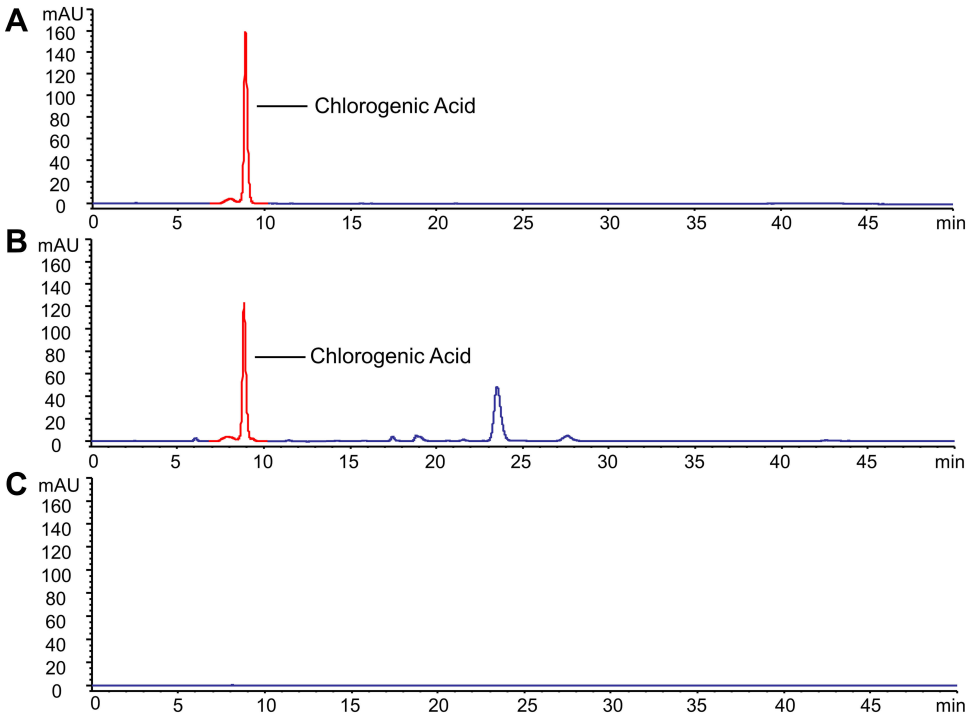

Figure 5 High-performance liquid chromatography (HPLC) profile of (**A**) chlorogenic acid, (**B**) *Lonicerae japonicae* Flos (LJF), and (**C**) *Lonicerae japonicae* Flos carbonisata-derived carbon dots (LJFC-CDs).

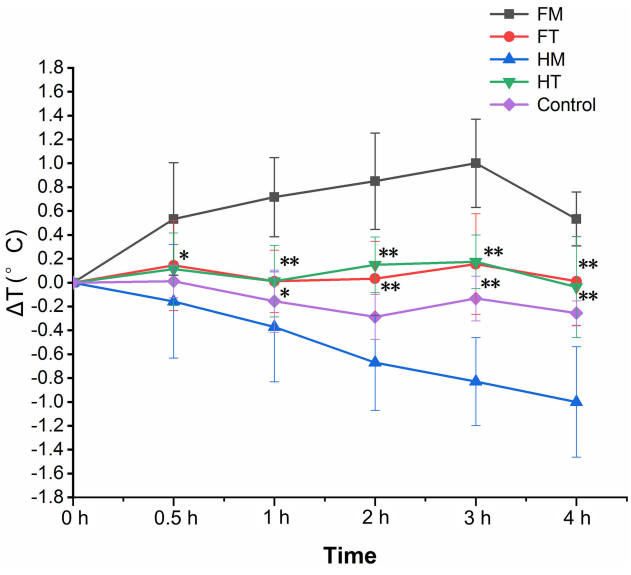

Figure 6 The mean body temperature of rats in the fever model (FM), fever treatment (FT), hypothermia model (HM), hypothermia treatment (HT), and control groups (x ± s, n = 8). FT group: *$p < 0.05$, **$p < 0.01$ vs FM group; HT group: *$p < 0.05$, **$p < 0.01$ vs HM group.

Effect of LJFC-CDs on Inflammatory Cytokines in Serum

Compared with those in the control group, serum concentrations of TNF-α (Figure 7A) in the FM (56.63 ± 6.09 pg/mL) and HM (63.75 ± 13.60 pg/mL) groups were significantly increased. Compared with those in the FM group, serum TNF-α concentrations were higher in the HM group. The serum concentrations of TNF-α in the FT (26.35 ± 7.12 pg/mL) and HT (27.45 ± 7.83 pg/mL) groups were close to those in the control (20.27 ± 4.21 pg/mL) group, and lower than those in the two model groups ($p < 0.01$). Similarly, the concentrations of IL-1β (Figure 7B) in the FM (31.28 ± 6.49 pg/mL) and HM (42.10 ± 8.04 pg/mL) groups also increased. There were significant differences between the FT (18.66 ± 3.70 pg/mL) and the FM groups, and the HT (21.36 ± 4.59 pg/mL) and HM ($p < 0.01$) groups. Additionally, the concentrations of IL-1β in both treatment groups were similar to those in the control (14.67 ± 4.99 pg/mL) group. The concentrations of IL-6 (Figure 7C) in the control group were 13.95 ± 2.42 pg/mL. Compared with those on the FM (28.12 ± 3.89 pg/mL) group, the concentrations of IL-6 in the FT (15.12 ± 2.33 pg/mL) group were significantly lower ($p < 0.01$). The concentrations of IL-6 were higher in the HM (41.37 ± 6.58 pg/mL) group compared with those in the FM group. The concentrations of IL-6 in the HT (17.68 ± 2.28 pg/mL) group were significantly reduced following oral administration of LJFC-CDs ($p < 0.01$).

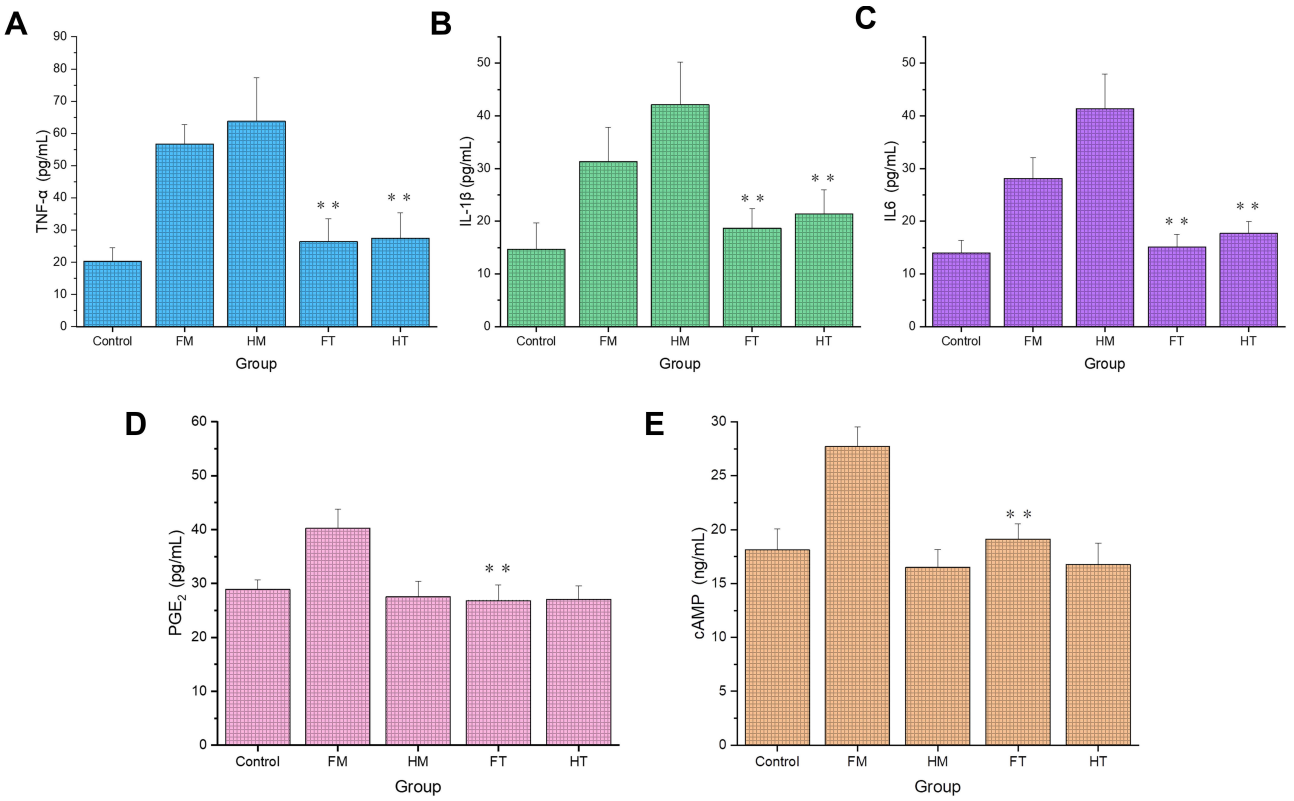

Figure 7 Serum concentrations of (**A**) tumor necrosis factor (TNF)-α; (**B**) interleukin (IL)-1β; and (**C**) IL-6. The concentrations of (**D**) PGE_2 and (**E**) cAMP in the preoptic anterior hypothalamus (PO/AH). FT group: $^{**}p < 0.01$ vs FM group; HT group: $^{**}p < 0.01$ vs HM group.

Effect of LJFC-CDs on PGE_2 and cAMP in PO/AH

The concentration of PGE_2 in the PO/AH (Figure 7D) was significantly higher in the FM (40.28 ± 3.54 pg/mL) group compared with those in the other four groups ($p < 0.01$). Including the HM (26.82 ± 2.90 pg/mL) group, there were little differences among the four groups. Additionally, the concentrations of cAMP (Figure 7E) in the FT (19.12 ± 1.40 ng/mL) group were significantly different from those in the FM (27.70 ± 1.83 ng/mL) group ($p < 0.01$).

Discussion

Research on charcoal medicine in TCM has long focused on hemostasis, which is closely related to TCM empirical theory. However, studies (other than those evaluating effects on hemostasis) on charcoal-processed drugs are limited. Through preliminary work, our research group has demonstrated that CDs are the material basis for the activity of carbon drugs.[11–14] We have reported that the carbonisata-derived CDs of drugs such as *Junci Medulla*,[15] *Schizonepetae Spica*,[16] *Phellodendri Cortex*,[13] and *Pollen Typhae*[17] have promising hemostatic bioactivity. Moreover, our group has identified that other applications of carbon nano-ingredients, for example, *mulberry silkworm* cocoon-derived carbon dots possess anti-inflammatory;[18] *Jiaosanxian* carbonisata-derived CDs were found to effectively regulate blood sugar;[19] and *Puerariae lobatae* Radix carbonisata-derived CDs were shown to possess anti-gout activity.[20] Therefore, our follow-up research is more focused on other applications (other than hemostasis) of charcoal-processed drugs.

LJF is a kind of Chinese herbal medicine, that is effective for heat-clearing and detoxifying materials, and possesses antibacterial, antiviral, and antipyretic properties. Hence, LJF is commonly used to treat fever, carbuncle, tumors, and other diseases. LJFC is preferred for detoxifying (relieving fever, inflammation and other symptoms). Active small molecule compounds, such as chlorogenic acid, are considered pharmacologically active components of LJF. Based on our previous work and the efficacy of LJFC, we evaluated the effect of LJFC-CDs on LPS-induced fever and hypothermia in rats.

In this study, LJF was used to prepare LJFC-CDs via one-step pyrolysis. This preparation method has advantages of using green raw materials, being a simple operation that is easy to control, and having environmentally

friendly processing. LJFC-CDs were characterized and identified by TEM, HRTEM, FIIR, UV–vis spectroscopy, fluorescence spectroscopy, XPS, and XRD. Concurrently, LJF and LJFC-CDs solutions were compared and evaluated by HPLC; LJFC-CDs were found to contain no active small molecule compounds, such as chlorogenic acid. This is in line with our previous studies, which have confirmed that the active small molecule compounds are removed after the drug is carbonized, but these remaining carbonisata-derived CDs still play a role.[13,15–17]

Herein, we found that the LJFC-CDs could reduce the level of inflammatory factors and regulate abnormal body temperature induced by LPS. The detection data of cytokines in serum and the changes in body temperature strongly supported this result.LPS, an endotoxin, is commonly used to establish systemic inflammatory models. Systemic inflammatory response is usually accompanied by fever or hypothermia.[21] LPS-induced fever is caused by inflammation, followed by the rapid production of PGE_2.[22] Previous studies have demonstrated that LPS-induced hypothermia is associated with TNF-α.[23] In the hypothermia caused by systemic inflammation, TNF-α functions as an endogenous cryogen.[24] As a consequence of increased levels of inflammatory cytokines, such as TNF-α, IL-1β, and IL-6, PGE_2 generation is promoted under low-dose LPS conditions. Therefore, fever was observed in the FM group. Serum concentrations of TNF-α, IL-1β, and IL-6 in rats of the FM group increased, and the concentrations of PGE_2 and cAMP in the PO/AH region followed a similar trend. Under conditions of high-dose LPS, higher concentrations of TNF-α, IL-1β, and IL-6 triggered self-preservation, resulting in hypothermia. Therefore, compared with rats in the FM group, those in the HM group presented higher TNF-α, IL-1β, and IL-6 concentrations. The occurrence of fever indicates high levels of inflammatory cytokines and consequently, generation of high levels of PGE_2. However, concentrations of PGE_2 and cAMP in the PO/AH region of rats in the HM group were maintained at normal levels. This is difficult to explain and may reflect the action of other cytokines not studied here, or the effect of a temperature "setpoint" in the body. It is also possible that changes in body temperature affect the concentrations of PGE_2 and cAMP, rather than their concentrations affecting body temperature.

Additionally, the concentrations of TNF-α, IL-1β, IL-6, PGE_2, and cAMP in the two treatment groups were not significantly different from those in the control group. This indicates that LJFC-CDs could regulate LPS-induced abnormal body temperature by clearing TNF-α, IL-1β, and IL-6. Drugs may cross the blood-brain barrier (BBB) via lipid-mediated free diffusion, providing the drug has a molecular weight <400 Da and forms <8 hydrogen bonds, which are lacking in all large molecule drugs.[25] Since the diameters of LJFC-CDs ranged from 1.0 to 10.0 nm, they are unable to cross the BBB. Therefore, in the FT group, LJFC-CDs controlled the increase in body temperature by reducing the levels of TNF-α, IL-1β, and IL-6 in serum and further blocking the production of PGE_2. Concurrently, the concentration of cAMP also decreased. In the HT group, hypothermia was caused by the increase of TNF-α. Consequently, body temperature was kept stable owing to the clearance of TNF-α by LJFC-CDs. These results suggest that LJFC-CDs regulated LPS-induced fever by reducing TNF-α, IL-1β, and IL-6 in serum, and hypothermia by reducing TNF-α from the serum.

Inflammation often triggers changes in body temperature. Multiple factors and mechanisms can result in abnormal body temperature. Inflammation is one of the common factors causing fever or hypothermia; but many studies have focused on fever rather than hypothermia. Many antipyretic drugs, such as ibuprofen and acetaminophen, with potent and rapid effects, have been developed for clinical use. However, the mechanism underlying the development of hypothermia is unknown; there are few therapeutic methods and most involve heating by physical methods. This may be due to hypothermia is not common, and warm keeping is the best measure to treat hypothermia caused by cold and trauma. Meanwhile, hypothermia, caused by systemic inflammation, comes from severe diseases such as septicemia, and the focus of treatment is not on the body temperature. Even so, hypothermia caused by inflammation, like fever, is worth studying. LPS is a component of Gram-negative bacteria. Pseudomonas aeruginosa, Yersinia pestis, Shigella dysenteriae are also belonging to Gram-negative bacteria; pneumonia caused by Pseudomonas aeruginosa, plague caused by Yersinia pestis, dysentery caused by Shigella dysenteriae and some other diseases not only have inflammatory reaction, but also have fever or hypothermia with the change of disease condition.

LJFC-CDs were able to remove TNF-α, IL-1β, and IL-6, indicating their potential for reducing inflammation and regulating body temperature abnormalities caused by inflammation. This study provides preliminary evidence for the anti-inflammatory of LJFC-CDs and its ability to relieve fever or hypothermia caused by inflammation; however, further studies are required to determine the underlying mechanisms and bioactivities.

Conclusion

In this study, we have successfully synthesized LJF into LJFC-CDs with low toxicity by one-step pyrolysis. To the best of our knowledge, for the first time, this study proves that the LJFC-CDs could reduce fever and hypothermia induced by LPS, and relieve inflammation by reducing the concentrations of TNF-α, IL- 1β and IL-6 in serum. This suggests the potential of LJFC-CDs as a drug with anti-inflammatory effect and for restoring abnormal body temperature triggered by inflammation.

Acknowledgments

We greatly appreciate the support of the National Natural Science Foundation (grant number 81573573) and the Classical Prescription Basic Research Team of the Beijing University of Chinese Medicine.

Disclosure

The authors declare that they have no known competing financial interests or personal relationships that could have appeared to influence the work reported in this paper.

References

1. Mishra V, Patil A, Thakur S, Kesharwani P. Carbon dots: emerging theranostic nanoarchitectures. *Drug Discov Today*. 2018;23(6):1219–1232. doi:10.1016/j.drudis.2018.01.006
2. Jaleel JA, Pramod K. Artful and multifaceted applications of carbon dot in biomedicine. *J Controlled Release*. 2018;269:302–321. doi:10.1016/j.jconrel.2017.11.027
3. Khajuria DK, Kumar VB, Gigi D, Gedanken A, Karasik D. Accelerated bone regeneration by nitrogen-doped carbon dots functionalized with hydroxyapatite nanoparticles. *ACS Appl Mater Interfaces*. 2018;10(23):19373–19385. doi:10.1021/acsami.8b02792
4. Devi P, Saini S, Kim KH. The advanced role of carbon quantum dots in nanomedical applications. *Biosens Bioelectron*. 2019;141:111158.
5. Norouzi M, Amerian M, Amerian M, Atyabi F. Clinical applications of nanomedicine in cancer therapy. *Drug Discov Today*. 2020;25(1):107–125. doi:10.1016/j.drudis.2019.09.017
6. National Pharmacopoeia Committee. *Pharmacopeia of the People's Republic of China 2015*. Beijing: Chinese Pharmacopeia Commission; 2015.
7. Su J *Xin Xiu Ben Cao*. Shanghai: Shanghai Ancient Books Publishing House; 1985.
8. Su S. *Su Shen Liang Fang*. Beijing: ChinaMedical Science Press; 2019.
9. Garami A, Steiner AA, Romanovsky AA. Fever and hypothermia in systemic inflammation. *Handb Clin Neurol*. 2018;157:565–597.
10. Wang S, Zhang Y, Kong H, et al. Antihyperuricemic and anti-gouty arthritis activities of Aurantii fructus immaturus carbonisata-derived carbon dots. *Nanomedicine*. 2019;14(22):2925–2939. doi:10.2217/nnm-2019-0255
11. Zhao Y, Zhang Y, Qin G, et al. In vivo biodistribution and behavior of CdTe/ZnS quantum dots. *Int J Nanomedicine*. 2017;12:1927–1939. doi:10.2147/IJN.S121075
12. Zhang M, Zhao Y, Cheng J, et al. Novel carbon dots derived from schizonepetae herba carbonisata and investigation of their haemostatic efficacy. *Artif Cells Nanomed Biotechnol*. 2018;46(8):1562–1571. doi:10.1080/21691401.2017.1379015
13. Liu X, Wang Y, Yan X, et al. Novel Phellodendri Cortex (Huang Bo)-derived carbon dots and their hemostatic effect. *Nanomedicine*. 2018;13(4):391–405. doi:10.2217/nnm-2017-0297
14. Zhao Y, Zhang Y, Liu X, et al. Novel carbon quantum dots from egg yolk oil and their haemostatic effects. *Sci Rep*. 2017;7(1):4452. doi:10.1038/s41598-017-04073-1
15. Cheng J, Zhang M, Sun Z, et al. Hemostatic and hepatoprotective bioactivity of junci medulla carbonisata-derived carbon dots. *Nanomedicine*. 2019;14(4):431–446. doi:10.2217/nnm-2018-0285
16. Sun Z, Lu F, Cheng J, et al. Haemostatic bioactivity of novel schizonepetae spica Carbonisata -derived carbon dots via platelet counts elevation. *Artif Cells Nanomed Biotechnol*. 2018;46(sup3):308–317. doi:10.1080/21691401.2018.1492419
17. Yan X, Zhao Y, Luo J, et al. Hemostatic bioactivity of novel pollen typhae carbonisata-derived carbon quantum dots. *J Nanobiotechnology*. 2017;15(1):60. doi:10.1186/s12951-017-0296-z
18. Wang X, Zhang Y, Kong H, et al. Novel mulberry silkworm cocoon-derived carbon dots and their anti-inflammatory properties. *Artif Cells Nanomed Biotechnol*. 2020;48(1):68–76. doi:10.1080/21691401.2019.1699810
19. Sun Z, Lu F, Cheng J, et al. Hypoglycemic bioactivity of novel eco-friendly carbon dots derived from traditional chinese medicine. *J Biomed Nanotechnol*. 2018;14(12):2146–2155. doi:10.1166/jbn.2018.2653
20. Wang X, Zhang Y, Zhang M, et al. Novel carbon dots derived from puerariae lobatae radix and their anti-gout effects. *Molecules*. 2019;24(22):4152. doi:10.3390/molecules24224152
21. Romanovsky AA, Almeida MC, Aronoff DM, et al. Fever and hypothermia in systemic inflammation: recent discoveries and revisions. *Front Biosci*. 2005;10(1–3):2193–2216. doi:10.2741/1690
22. Roth J, Blatteis CM. Mechanisms of fever production and lysis: lessons from experimental LPS fever. *Compr Physiol*. 2014;4:1563–1604.
23. Derijk RH, Berkenbosch F, Offermanns S, Rosenthal W, Classen M, Schepp W. Hypothermia to endotoxin involves the cytokine tumor necrosis factor and the neuropeptide vasopressin in rats. *Am J Physiol*. 1994;266(5 Pt 1):G775–G782. doi:10.1152/ajpgi.1994.266.5.G775
24. Leon LR. Hypothermia in systemic inflammation: role of cytokines. *Fron biosci*. 2004;9:1877–1888. doi:10.2741/1381
25. Pardridge WM. Drug transport across the blood-brain barrier. *J Cereb Blood Flow Metab*. 2012;32(11):1959–1972. doi:10.1038/jcbfm.2012.126